Bronchoscopic Probe-Based Confocal Laser Endomicroscopy to Diagnose Diffuse Parenchymal Lung Diseases

Edith Silbernagel[1], Elvira Stacher-Priehse[2], Julien Dinkel[3,6,11], Herbert Stepp[7], Wolfgang Gesierich[8], Michael Lindner[4], Juergen Behr[5,11], Frank Reichenberger[8,10]

[1]Pneumology Clinic Altenmark / Pongau, Austria; [2]Department of Pathology, Asklepios Lung Center Munich-Gauting, Germany; [3]Department of Radiology, Asklepios Lung Center Munich-Gauting, Germany; [4]Department of Thoracic Surgery, University Hospital Salzburg, Austria; [5]Department of Internal Medicine V, Ludwig-Maximilians-University of Munich, Germany; [6]Department of Radiology, Ludwig-Maximilians-University of Munich, Germany; [7]Laser Research Laboratory, LIFE-Center, Ludwig-Maximilians-University of Munich, Germany; [8]Department of Pneumology, Asklepios Lung Center Munich-Gauting, Germany; [10]Department of Pneumology, Augustinum Hospital Munich, Germany; [11]Comprehensive Pneumology Center (CPC-M), University Hospital, LMU Munich, Helmholtz Zentrum München, Member of the German Center for Lung Research (DZL), Munich, Germany

Abstract. *Background:* Diagnosis of diffuse parenchymal lung disease (DPLD) is based on clinical evaluation, radiological imaging and histology. However, additional techniques are warranted to improve diagnosis. *Aims and objective:* Probe based confocal laser endomicroscopy (pCLE) allows real time in vivo visualisation of the alveolar compartment during bronchoscopy based on autofluorescence of elastic fibres. We used pCLE (Cellvizio®, Mauna Kea Technology. Inc, Paris, France) to characterise alveolar patterns in patients with different types of DPLD. *Methods:* In this pilot study we included 42 therapy naive patients (13 female, age 72.6 +/- 2.3 years), who underwent bronchoscopy for workup of DPLD. pCLE images were obtained during rigid bronchoscopy in affected lung segments according to HR-CT scan, followed by cryobiopsies in the identical area. Diagnoses were made by a multidisciplinary panel. The description of pCLE patterns was based on the degree of distortion of the hexagonal alveolar pattern, the density of alveolar structures, the presence of consolidations or loaded alveolar macrophages (AM). The assessment was performed by 2 investigators blinded for the final diagnosis. *Results:* The normal lung showed a typical alveolar loop pattern. In amiodarone lung disease loaded AM were predominant. COP showed characteristic focal consolidations. IPF was characterized by significant distortion and destruction, NSIP showed significant increase in density, and chronic HP presented with consolidations, mild distortion and density. *Conclusion:* pCLE shows potential as an adjunctive bronchoscopic imaging technique in the differential diagnosis of DPLD. Structured and quantitative analysis of the images is required.

Key words: interstitial lung disease, diffuse parenchymal lung disease, bronchoscopy, probe-based confocal laser endomicroscopy, imaging

Diffuse parenchymal lung diseases (DPLD) comprise a variety of diseases of the interstitial and the alveolar compartment of different etiologies. At present, the diagnosis is based on clinical, radiological and histological criteria in the context of a multidisciplinary discussion (1, 2, 3).

Imaging of the lung tissue is one of the major diagnostic procedures in DPLD, and high resolution thoracic computed tomography (HRCT) is currently

the method of choice (4-6). However, HRCT is often non-diagnostic in distinct forms of interstitial lung disease by providing only a low probability assessment (6). Approximately 60 % of patients with usual interstitial pneumonia (UIP) pattern on surgical lung biopsy do not show typical UIP pattern on HRCT. As a result, it would be valuable to consider additional imaging methods (7, 8).

Bronchoscopy is often used in the assessment of DPLD, mainly for collection of histological specimen in the advent of bronchoscopic cryobiopsy (9). While inspection of the tracheobronchial tree is mandatory during bronchoscopy, visualization of the alveolar compartment is not possible with standard bronchoscopic techniques.

Probe-based confocal laser endomicroscopy (pCLE) enables in vivo visualization of tissue in high resolution. A fiberoptic miniprobe excites autofluorescence of elastic tissue structures by emitting laser light with a wave length of 488nm (10).

Mainly employed in gastrointestinal and bile duct endoscopy, it has been also used to visualize lung tissue in vivo in health and disease, especially in tracheobronchial diseases and pulmonary diseases including infections with aspergillus and pneumocystis (11-15). Several imaging patterns have been described for distinct interstitial lung diseases, especially amiodarone lung disease and alveolar proteinosis as well as lung emphysema (16-22). However, there are sparse data exploring its use in the differentiation of idiopathic interstitial pneumonias (IIP) (23).

We explored the role of pCLE to assess different DPLD in real time during bronchoscopy, in order to describe distinct pCLE imaging patterns of the lung parenchyma, particularly with respect to the underlying disease and correlation with physiological parameters.

Materials and Methods

This is a single center prospective proof of concept study on use of bronchoscopic pCLE in the assessment of DPLD. We included patients referred for workup of newly diagnosed DPLD. All patients were age >18 years, in a stable clinical condition with no evidence of a current infection and not requiring oxygen supplement.

Each patient was assessed according to current guidelines including radiology with high resolution computed tomography scan (HRCT), laboratory parameters including antibodies and precipitins as outlined below and pulmonary function test including blood gas analysis and 6-minute-walk test. In addition, all subjects received a structured questionnaire for DPLD (24).

Pulmonary function test (PFT) and blood gas analysis (BGA)

Each patient underwent PFT including single-breath diffusing capacity for carbon monoxide corrected for hemoglobin (DLCOc-SB) and blood gas analysis at rest as well as a lung volume measurement using body plethysmography (Carefusion version V2.19.4, Höchberg, Germany). BGA was performed using arterialized capillary blood samples from the hyperaemic earlobe (Radiometer ABL 800flex).

Furthermore, all patients performed a six-minute walk test according to current guidelines (25).

Laboratory Tests

All patients received a basic laboratory assessment including differential cell count, liver/kidney function tests and CRP. Additionally, in all patients we measured anti nuclear antibodies, anti neutrophilic cytoplasmatic antibodies, rheumatoid factor and CCP- antibodies as well as IgG antibodies against aspergillus spp., thermoactinomyces spp, micopolyspora spp, and dove / budgerigar feathers.

Patients were excluded due to severe restrictive lung disease (VC or TLC below 50% pred.), severe hypoxaemia (pO2 < 55 mmHg on air), inborn or acquired disorder of the coagulation system, signs of pulmonary hypertension on echocardiography, ECG and brain natriuretic peptide according to current guidelines (26) or inability to undergo bronchoscopy for any medical or legal reason.

All patients gave written informed consent 24 hours prior to the bronchoscopy examination. All patients obtained information by a respiratory physician and gave their written informed consent for the use of the pCLE confocal miniprobe during the routine bronchoscopy. The patient was informed about side effects post procedure, particularly bleeding and pneumothorax.

The study was approved by the local ethics committee of the Ludwig Maximilians University Munich, Germany, (Record number 048/13).

Bronchoscopy and pCLE

Bronchoscopy was performed in rigid technique in general anesthesia. After intubation, flexible bronchoscopy (BF-Q 180, Olympus, Japan) was used for inspection of the bronchial tree and to collect mucus samples for microbiological and cytological examinations. Afterwards, the specific miniprobe (AlveoFlex, Cellvizio, Mauna Kea Technologies, France) with a diameter of 1.4mm twice the size of an alveolar duct was inserted via the bronchoscopic working channel (Figure 1). The miniprobe excites autofluorescence of elastic tissue structures by emitting laser light with a wave length of 488nm. It has a depth of focus of 0-50 μm, a lateral resolution of 3.5 μm for a field of view of 600 μm diameter. Images were recorded with a frame rate of 12 images per second. No exogenous fluorophores were applied. The probe was pushed forward alongside the bronchial tree in the peripheral compartment under fluoroscopic guidance until the elastic fibres of the alveolar structure were identified. At this stage we recorded a short video sequence of one minute.

In every patient we performed pCLE imaging in the most prominent and affected lung areas according to HRCT scan, that were accessible for placement of pCLE probe. This includes segment 2 or 3 in the upper lobe, the middle lobe or the lingula, and preferably lateral subsegment of segment 8, or segment 9 in the lower lobes. If no appropriate images could be retrieved from the privileged subsegments, we examined the neighboring subsegment.

For histology, we performed 3 cryobiopsies using a 19 mm cryoprobe to obtain a sufficient tissue

Figure 1. Flexible bronchoscope (6 mm outer diameter) with pCLE probe in the working channel

specimen from the identical lung segment which had been examined by pCLE. The freezing time was 2 seconds at the first freezing procedure. If no sufficient specimen could be obtained, the freezing time has been expanded to 3 seconds. Afterward, bronchoalveolar lavage (BAL) was performed in the middle lobe or the lingula using 120 mls of 0.9% saline for cytological evaluation. Post bronchoscopy all patients received a chest- X- ray to exclude a pneumothorax. Histology samples were analysed by a pathologist specialized in lung diseases.

Diagnosis of DPLD

Each patient was discussed in the multidisciplinary pneumology- radiology- pathology ILD board to make a final diagnosis of the DPLD (3, 5).

pCLE Image Acquisition, Processing and Evaluation

The assessment was performed in a team of 2 investigators blinded to clinical data as well as results of diagnostic workup and the final diagnosis of the multidisciplinary ILD- board (ES and FR), using Cellvizio Viewer Software version 1.6.0 (Mauna Kea technologies, France).

Firstly, the pCLE video sequences were reviewed to analyse the most prevalent changes and findings. Based on these experiences we described four categories of findings that involves degree of distortion of the hexagonal alveolar pattern, density of alveolar structures, focal consolidations, and presence of loaded alveolar macrophages.

Afterwards, the pCLE video sequences were semi- quantitatively assessed. Therefore, we developed a four- scale evaluation system for each category from "0"- no presence of changes to "3" significant presence of changes in every category mentioned above. Example images are shown in figure 2.

Finally, the results of the assessment were matched with the DPLD diagnoses of the MDD.

Results

Diagnosis of DPLD

Between November 2013 and November 2016 we included 42 patients with newly diagnosed DPLD. Five non- smoking patients with normal

PFT and lung parenchyma on HRCT but an additional indication for bronchoscopy served as normal controls.

All patients were diagnosed according to clinical, radiological and histological findings after multidisciplinary team discussion (table 1)

Bronchoscopy and Side Effects

Bronchoscopies were well tolerated, and all patients were extubated after the procedure.

During the diagnostic procedures including transbronchial cryobiopsies, there were minor

Consolidation
areas of localized thickening of alveolar structures

| Grade 0 | Grade 1 | Grade 2 | Grade 3 |

Loaded Alveolar macrophages
Presences of loaded cell components

| Grade 0 | Grade 1 | Grade 2 | Grade 3 |

Distortion
Disruption of normal alveolar loop architecture and replacement by disordered fibre- like structures

| Grade 0 | Grade 1 | Grade 2 | Grade 3 |

Density

Increased quantity of fibre- like structures with partially preserved alveolar loops

Grade 0   Grade 1   Grade 2   Grade 3
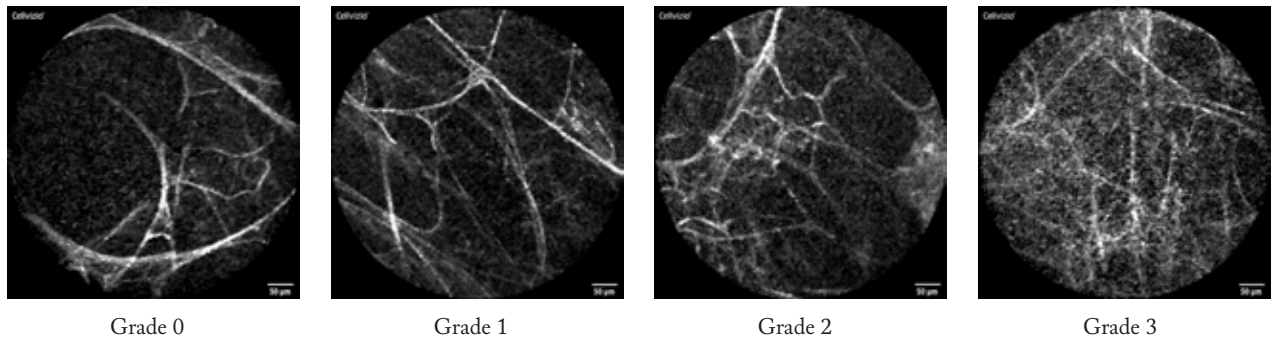
Figure 2. 4 items sample images for semi- quantitative analysis using a 4- degree score (0-3) images were obtained from patients included in the study

Table 1. Patients characteristics, pulmonary function tests and GAP score in respect to the underlying disease in mean (SD)

	Gender m/f	Age (SD)	VC (L)	VC (%)	TLC (L)	TLC (%)	DLCO c-SB (%)	P02 mmHg	PC02 mmHg	GAP
COP	*8/2*	69 (11)	3.36 (0.9)	88.5 (18.3)	5.81 (1.1)	90.1 (21.9)	69.16 (19.1)	70.93 (8.3)	35.27 (3.0)	3.1 (1.19)
NSIP	*5/5*	72 (6.0)	2.34 (0.8)	77.3 (16.4)	4.58 (1.0)	82.2 (13.7)	45.38 (17.8)	67.02 (8.5)	35.32 (2.4)	3.9 (1.4)
Chronic HP	*6/2*	71 (5.4)	2.58 (0.8)	74.61 (25.0)	4.37 (1.0)	71.83 (22.5)	46.75 (14.6)	72.31 (13.0)	34.30 (3.7)	4 (1.6)
IPF	*6/3*	73 (4.9)	2.27 (0.8)	66.02 (20.3)	4.14 (0.7)	67.02 (8.3)	41.06 (17.0)	63.77 (8.4)	40.75 (2.86)	4.77 (1.6)
AMR-IP	*4/1*	72 (9.3)	2.87 (0.7)	67.46 (17.9)	5.18 (0.9)	72.18 (14.6)	35.5 (7.5)	57.68 (5.3)	32.2 (2.0)	5 (2)
Total mean (SD)	*n=42*	72.62 (2.31)	2.61 (0.21)	72.36 (4.87)	4.67 (0.23)	75.41 (5.9)	48.52 (3.55)	67.14 (2.87)	35.73 (0.58)	4.32 (0.33)

bleedings that could be stopped by bronchoscopic means, but none of the patients required endobronchial tamponade or balloon blockage, prolonged ventilation, transfusion, or radiological/surgical interventions.

In 9 patients we diagnosed a postinterventional pneumothorax (22%), most likely caused by transbronchial cryobiopsy. These patients required a thoracic drainage for 3.6 (1.2) days. All pneumothoraces occurred during the first 15 examinations.

None of the patients experienced a postinterventional exacerbation or infection during the further hospital stay of mean 1 ½ days.

pCLE-Patterns

The pCLE video sequences were assessed semi-quantitatively using the prespecified four categories (distortion, density, consolidation, presence of loaded alveolar macrophages (AM)). The semi- quantitative image analysis was performed by a 4- degree score according to representative sample images (figure 2).

Table 2 shows the results in respect to the underlying clinical disease.

We could describe distinct pCLE patterns in respect to the underlying lung disease (figure 3 a-f)

pCLE of Normal Alveolar Tissue

In patients with normal lung imaging, we found fine alveolar septal structures with separated loop characteristics and minimal blurring reflexes representing secretions, but no macrophages or architectural distortion were noted (see images distortion 0, density 0, AM 0, consolidation 0). (figure 3 a)

Table 2. pCLE assessment with respect to the underlying disease. pCLE features and assessment in the 4- degree- scale shown as mean (number of individual values of every degree below)

	Distortion	Density	Loaded AM	Consolidation
	Mean	Mean	Mean	Mean
	(0/1/2/3)	(0/1/2/3)	(0/1/2/3)	(0/1/2/3)
COP	1	1.75	0	1.1
	(3/5/2/0)	(0/5/4/1)	(8/2/0/0)	(1/7/2/0)
NSIP	1.2	1.9	0.9	1.1
	(2/5/3/0)	(0/3/5/2)	(6/1/1/2)	(3/4/2/1)
Chronic HP	1	1.81	0.25	1
	(2/5/1/0)	(0/2/6/0)	(6/2/0/0)	(1/6/1/0)
IPF	2	2.38	0.11	0.88
	(0/3/3/3)	(1/0/3/5)	(8/1/0/0)	(3/4/2/0)
AMR-IP	1.1	1.6	1.6	0.2
	(1/3/1/0)	(0/3/1/1)	(2/0/1/2)	(4/1/0/0)

pCLE Pattern in Cryptogenic Organizing Pneumonia (COP)

Typical for this condition is a higher density and the presence of focal consolidations. The alveolar structure remains thin. Heterogeneity was markedly increased, but the structures did not show a significantly increased distortion. No loaded AM were detected (figure 3 b)

pCLE Pattern in Nonspecific Interstitial Pneumonia (NSIP)

NSIP-images are characterized by a significant increase in density. The alveolar structures are thickened but in normal configuration. They showed a characteristic crystalline coating with "gloss like" reflections. In cellular NSIP loaded cells smaller than AM were detected, while AM were not present. Only minor distortion and consolidation were noted. (figure 3 c)

pCLE Pattern in Chronic Hypersensitivity Pneumonitis (HP)

In this category we did find mainly consolidations with mildly increased distortion and density, but no loaded AM. Other features appear to correlate with the histological subtypes, e.g. fibrotic or cellular HP. (figure 3 d)

pCLE pattern in Idiopathic Pulmonary Fibrosis (IPF)

In IPF, the pCLE pattern is characterized by a severe distortion and destruction of the alveolar structures and increased density with a "hair- perm" like pattern in the most severe cases. In 3 cases with active smoking, we could detect loaded AM (case 7, 12, 16). Minor findings included consolidation and local changes. (figure 3 e)

pCLE Pattern in Amiodaron-Lung Disease

The hallmark of this ILD is the vast amount of loaded AM, which are situated like grape vine within the alveolar spaces. This is in contrast to active smokers, in whom increased numbers of loaded but freely floating AM were found. No other characteristic findings were observed. (figure 3 f)

pCLE and BAL

BAL results were compatible with the underlying DPLD (data not shown). Concerning pCLE, there was no correlation between BAL differential cell count and pCLE pattern in the whole patient group.

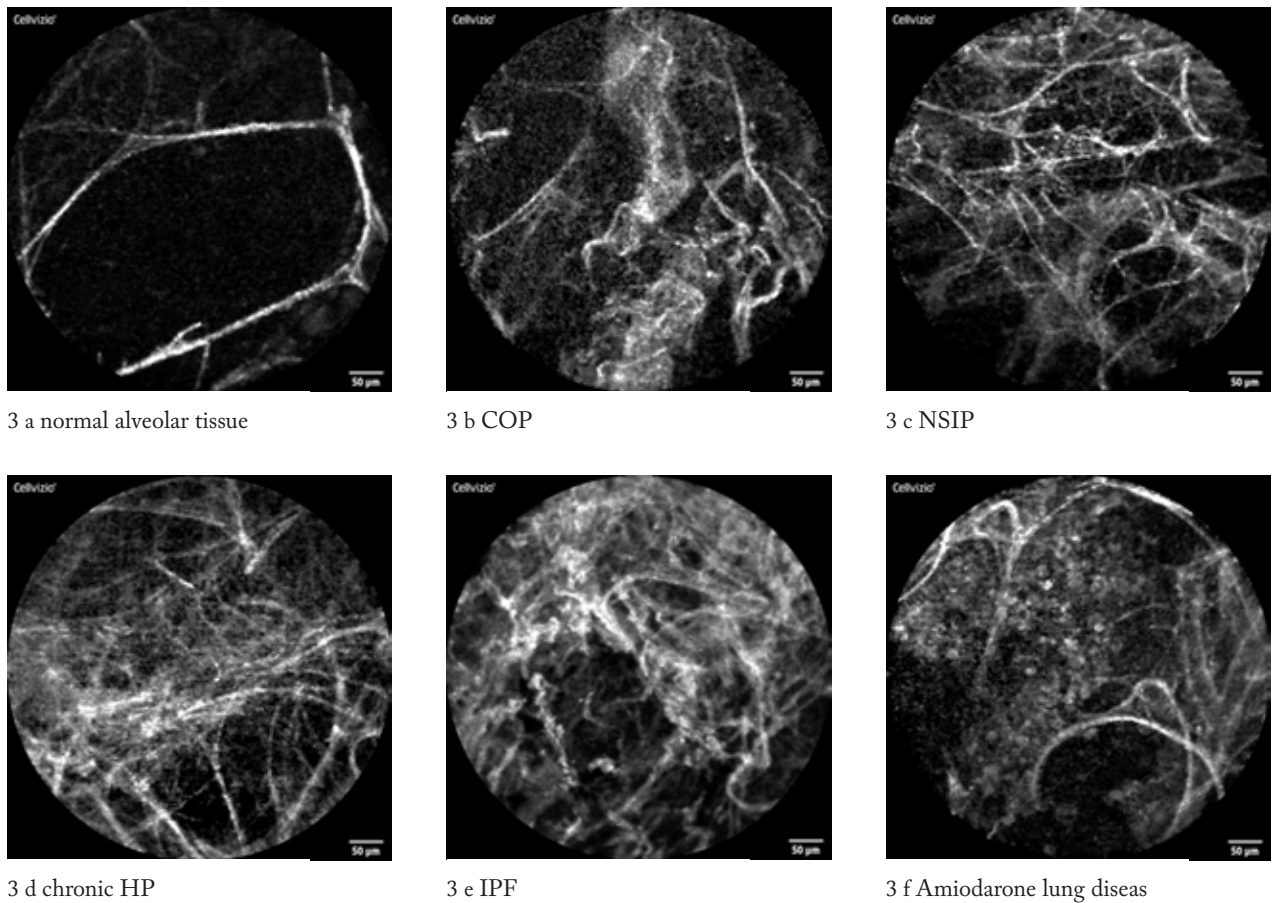## Pulmonary Function Test (PFT) and Clinical Performance Status (GAP Score)

The PFT showed a moderate restrictive pattern with a varying degree of impaired diffusion capacity as outlined in table 1. No patient showed a resting hypoxemia or hypercapnia at time of initial assessment. GAP score (27) showed a mild to moderate degree of clinical impairment
Neither PFT nor GAP score did show a significant correlation with pCLE results.

Discussion

The diagnosis of DPLD is a current hotspot in respiratory medicine. In this study we report our experience with pCLE in the assessment of DPLD.
While in normal lung typical alveolar loop patters were visible, in COP focal consolidations and

3 a normal alveolar tissue

3 b COP

3 c NSIP

3 d chronic HP

3 e IPF

3 f Amiodarone lung diseas

Figures 3 (a – f). pCLE images of DPLD according to MDD diagnosis images were obtained from patients included in the study

higher tissue density were present. IPF is characterized by significant distortion and destruction, while NSIP showed significant increase in density with "cristalline coating". In chronic HP there were mainly consolidations with mild distortion and density, while Amiodarone lung disease was characterized by loaded AM.

Based on these results we developed a 4- point 4- degree semi- quantitative evaluation scale to describe typical imaging patterns according to the underlying disease (table 2).

In our opinion, pCLE enables in vivo visualization of characteristic changes in respect of the underlying DPLD beyond the scope of radiological and histological examinations (13). In our study, pCLE did not detect specific histopathological findings such as fibroblast foci or interstitial inflammation. The pCLE technique uses a laser wavelength, that visualizes mainly elastic fibres but not collagen fibres in vivo, thus capturing parenchymal structure indirectly. Therefore, we regard pCLE as a separate imaging method and evaluated the pCLE images in respect to the final DPLD diagnosis rather than in comparison with single histology or radiology results.

So far, we used a semi- quantitative procedure for image analysis. Using this method, we could describe pCLE patterns predominantly present in distinct forms of DPLD. As there is no established procedure for evaluation of pCLE images, we developed an assessment based on a four category four scale system as shown in figure 1. Certainly, a significant subjective bias has to be considered and its usefulness has to be proven also in the follow-up. A better and more reproducible evaluation is required that also includes a quantitative analysis of the images (28). A first approach to a computerized image analysis has been recently published by our group (29)

In this pilot study we did not observe any association of pCLE findings with physiological parameters including PFT and GAP score. These might be influenced by the small sample size. The study was primarily focused on feasibility of the pCLE technique in DPLD and description of distinct patterns.

The handling of bronchoscopic pCLE probe was dependent on the alteration of the bronchial tree due to lung restriction. When the position of the bronchi is more horizontally and straight, this aggravates the accessibility of the lung parenchyma by the pCLE probe. We advanced the probe under fluoroscopy, until a parenchymal image has been obtained at maximum 1 cm subpleurally. Using these precautions, we did not observe any significant side effects such as bleeding or respiratory failure post bronchoscopy. However, we observed 9 pneumothoraces requiring drainage in the first 22 examinations. As the occurrence of pneumothorax might be a rare side effect of CLE (13), it could be caused by the cryobiopsy performed afterwards (30).

The pCLE procedure could be shortened during the study period from approximately 25 minutes at the beginning to approximately 10 minutes using the identical protocol. However, we did not use a time recording during the test to provide robust data.

In this study we performed the examination in rigid bronchoscopy due to our institutional safety measure when performing transbronchial cryobiopsies. However, pCLE can be easily and safely performed in flexible technique, as there is no increased safety concern.

Based on our experience we consider pCLE as an independent diagnostic procedure in DPLD beyond a guidance tool to direct transbronchial cryobiopsy as recently mentioned (31).

Our study is a proof- of- concept study with a relatively small patient population and a newly developed evaluation method. These findings need to be confirmed in larger patient populations concerning practicability of the method and their impact on diagnosis of DPLE beyond histology and radiology. Of note, we diagnosed 10 patients with idiopathic NSIP. This might be explained by a referral bias in our cohort, excluding patients with underlying causes of DPLD such as connective tissue diseases. Furthermore, we excluded patients with severe functional impairment including patients on long-term oxygen therapy due to safety reasons.

In conclusion, pCLE harbours the potential to serve as an in vivo bronchoscopic imaging technique in the assessment and differential diagnosis of ILD. The major challenges are obtaining a representative sample of pCLE images and their structured assessment.

References

1. Tomassetti S, Ravaglia, Poletti V. Diffuse parenchymal lung disease. Eur Respir Rev 2017;26(144).
2. Castillo D, Walsh S, Hansell DM, et al. ERICE ILD working group. Validation of multidisciplinary diagnosis in IPF. Lancet Respir Med 2018;6(2):88-89.
3. Travis WD, Costabel U, Hansell DM, et al. ATS/ERS Committee on Idiopathic Interstitial Pneumonias. An official American Thoracic Society/European Respiratory Society statement: Update of the international multidisciplinary classification of the idiopathic interstitial pneumonias. Am J Respir Crit Care Med 2013;188(6):733-48
4. Hodnett PA, Naidich DP. Fibrosing interstitial lung disease. A practical high-resolution computed tomography-based approach to diagnosis and management and a review of the literature. Am J Respir Crit Care Med 2013;188(2):141-9
5. Interstitial lung diseases in European Lung White Book, editors J Gibson, R Loddenkemper, Y Sibille, B Lundbäck. Part C, Chapter 22. Page 256- 269, 2013. www.erswhitebook.org.
6. Lynch DA, Sverzellati N, Travis WD, et al. Diagnostic criteria for idiopathic pulmonary fibrosis: a Fleischner Society White Paper. Lancet Respir Med 2018;6(2):138-153.
7. Martinez FJ, Chisholm A, Collard HR, et al. The diagnosis of idiopathic pulmonary fibrosis: current and future approaches. Lancet Respir Med 2017;5:61–71
8. Sgalla G, Kulkarni T, Antin-Ozerkis D, Thannickal VJ, Richeldi L.Update in Pulmonary Fibrosis 2018. Am J Respir Crit Care Med 2019;200(3):292-300
9. Hetzel J, Maldonado F, Ravaglia C, Wells AU, et al. Transbronchial Cryobiopsies for the Diagnosis of Diffuse Parenchymal Lung Diseases: Expert Statement from the Cryobiopsy Working Group on Safety and Utility and a Call for Standardization of the Procedure. Respiration 2018;95(3):188-200.
10. Thiberville L, Salaun M, Bourg-Heckly G. In vivo confocal microendoscopy: from the proximal bronchus down to the pulmonary acinus. Eur Respir Monogr 2010;48:73–89.
11. Thiberville L, Salaün M. Bronchoscopic advances: on the way to the cells. Respiration 2010;79(6):441-9.
12. Newton RC, Kemp SV, Yang GZ, Elson DS, Darzi A, Shah PL. Imaging parenchymal lung diseases with confocal endomicroscopy. Respir Med 2012;106(1):127-37.
13. Meng P, Tan GL, Low SY, Takano A, Ng YL, Anantham D. Fibred confocal fluorescence microscopy in the diagnosis of interstitial lung diseases. J Thorac Dis 2016; 8(12): 3505-3514.
14. Newton RC, Kemp SV, Yang GZ, Darzi A, Sheppard MN, Shah PL. Tracheobronchialamyloidosis and confocal endomicroscopy. Respiration 2011;82(2):209-11.
15. Danilevskaya O, Averyanov A, Lesnyak V, Chernyaev A, Sorokina A. Confocal laser endomicroscopy for diagnosis and monitoring

of pulmonary alveolar proteinosis. J Bronchology Interv Pulmonol 2015;22(1):33-40.

16. Salaün M, Roussel F, Bourg-Heckly G, et al. In vivo probe-based confocal laser endomicroscopy in amiodarone-related pneumonia. Eur Respir J 2013;42(6):1646-58.

17. Salaün M, Roussel F, Hauss PA, Lachkar S, Thiberville L. In vivo imaging of pulmonary alveolar proteinosis using confocal endomicroscopy. Eur Respir J 2010;36(2):451-3.

18. Morisse H, Heyman L, Salaün M, et al. In vivo molecular microimaging of pulmonary aspergillosis. Med Mycol 2013;51(4):352-60.

19. Shafiek H, Fiorentino F, Cosio BG, et al. Usefulness of Bronchoscopic Probe-Based Confocal Laser Endomicroscopy in the Diagnosis of Pneumocystis jirovecii Pneumonia. Respiration 2016;92(1):40-7.

20. Yserbyt J, Dooms C, Janssens W, Verleden GM. Endoscopic advanced imaging of the respiratory tract: exploring probe-based confocal laser endomicroscopy in emphysema. Thorax. 2018;73(2):188-190.

21. Shah PL, Kemp SV, Newton RC, Elson DS, Nicholson AG, Yang GZ. Clinical Correlation between Real-Time Endocytoscopy, Confocal Endomicroscopy, and Histopathology in the Central Airways. Respiration 2017;93(1):51-57. Epub 2016 Nov 18. PubMed PMID: 27855380.

22. Newton RC, Kemp SV, Shah PL, et al. Progress toward optical biopsy: bringing the microscope to the patient. Lung 2011;189(2):111-9. doi: 10.1007/s00408-011-9282-7. Epub 2011 Feb 20. Review. PubMed PMID: 21336942.

23. Salaün M, Guisier F, Dominique S, et al. In vivo probe-based confocal laser endomicroscopy in chronic interstitial lung diseases: Specific descriptors and correlation with chest CT. Respirology 2019: 783-791.

24. Kreuter M, Ochmann U, Koschel D, et al. DGP Interstitial Lung Disease Patient Questionnaire. Pneumologie 2018;72(6):446-457

25. Singh SJ, Puhan MA, Andrianopoulos V, et. al. An official systematic review of the European Respiratory Society/American Thoracic Society: measurement properties of field walking tests in chronic respiratory disease. Eur Respir J 2014;44(6):1447-78.

26. Guideline PH

27. Ley B, Ryerson CJ, Vittinghoff E, et al. A multidimensional index and staging system for idiopathic pulmonary fibrosis. Ann Intern Med 2012;156(10):684-91

28. Silbernagel E, Bondesson D, Behr J, Dinkel J, Reichenberger F. Taking Another View on Lung Fibrosis. Am J Respir Crit Care Med 2018; 197: 947-948.

29. Bondesson D, Schneider MJ, Silbernagel E, Behr J, Reichenberger F, Dinkel J. Automated evaluation of probe-based confocal laser endomicroscopy in the lung. PLoS One 2020;15(5):e0232847.

30. Poletti V, Ravaglia C, Tomassetti S. Transbronchial cryobiopsy in diffuse parenchymal lung diseases. Curr Opin Pulm Med 2016;22(3):289-96.

31. Wijmans L, Bonta PI, Rocha-Pinto R, et al. Confocal Laser Endomicroscopy as a Guidance Tool for Transbronchial Lung Cryobiopsies in Interstitial Lung Disorder. Respiration 2018:1-5.